SHALLOW-WATER SOUND TRANSMISSION MEASUREMENTS TAKEN ON THE NEW JERSEY CONTINENTAL SHELF

William M. Carey, James Doutt[a], Richard Evans[b], Lynne Dillman[c]

Advanced Research Projects Agency, 3701 North Fairfax Dr.
Arlington, Va. 22203

Abstract

Calibrated acoustic measurements were made under calm sea state conditions on the New Jersey shelf near the AMCOR 6010 borehole, a surveyed area with known geophysical properties. The experiment was conducted in 73 m water with supporting measurements of salinity, temperature, and sound speed. These measurements were obtained with a vertical array of 24 equally spaced hydrophones at 2.5 m; one of which was on the bottom. A source towed at either 1/2- or 3/4- water depth transmitted one of two sets of four tones spaced between 50 and 600 Hz for each run to ranges of 4 and 26 km. The data were processed with both a Hankel transform and a high resolution Doppler technique to yield horizontal wave-number spectrum at several depths. Results were obtained along both a constant and gradually varying depth radial. Similar modal interference patterns were observed at the lower frequencies. The constant depth radial results were compared to calculations performed with several shallow water acoustic models using geoacoustic profiles derived from geophysical parameters and shear wave inversion methods. Calculated and measured sound transmission results were found to agree when scattering within the sediment and between sedimentary layers was included. Range dependent radials were found to have effects consistent with sub-sediment acoustic features

1. Introduction

Shallow water sound transmission is said to be characterized by it's variability and reviews [1, 2] of this subject would seem to support this view. However, another characteristic of many shallow water experiments is the lack of knowledge of the environmental parameters such as the range dependent bottom, subbottom, depth, sound speed structure and sea state. Measurement system uncertainties have also been large and estimates of source-receiver depths, range and location have only recently been known accurately and subject to the experimenter's control. This is not to imply that careful shallow water experiments have not been performed because several have been [3-22], but rather to state that the objective of this work was to supplement these by performing a shallow water experiment under known and controlled conditions. The primary issues addressed in this experiment were the determination of the primary causes of sound transmission loss as a function of frequency (attenuation, shear waves, or scattering). A secondary objective was to examine the use of synthetic aperture processing as a shallow water survey method. The method chosen in this investigation was to build on the work of others whenever possible by using theory, numerical computer codes and measurement methods shown to be useful to supplement the measurement techniques developed for this investigation. The emphasis was to produce a calibrated set of transmission data with minimal and known uncertainties in the acoustic and environmental measurements.

The area chosen for this work was off the New Jersey Shelf. This is an area which has been extensively surveyed and is near a borehole (AMCOR 6010, [23, 24]) which provides the requisite knowledge of the geophysics parameters necessary to calculate the geoacoustic profiles [25-28], that is the compressional and shear wave speeds and attenuation constants as a function of depth . This area was also surveyed [29, 30] to yield a near surface characterization of the first 25m of sediment and identified the type of layering and sub-bottom reflectors such as the "R", "S", and "Channels". In addition two different shear modulus inversions were performed. The first by Stoll [31] used an impulsive shear wave source and a geophone array to measure the travel time curves which could used to determine the dispersion and with inversion techniques yielded the shear speed and attenuation profiles. The second by Yamamoto [32, 33] used the measurement of seabed motion and induced pressure due to the shallow water gravity waves coupled to an iterative inversion technique to estimate the shear modulus as function of sediment depth. These results provide a basis for the computation of the acoustic propagation characteristics in this shallow water wave guide.

Earlier work was based on the Pekeris theory [2,3,7] of the modal propagation in the a shallow water wave guide. This theory was developed for several analytical profiles and has been extended to other sound speed profiles [11]. This approach simply treats the sound propagation in a constant depth wave guide with multiple layers of liquids, in other words shear waves are ignored. However it provides a tractable analytical model useful for the qualitative design and conduct of an experiment such as this one. The details of the experimental were designed on the basis of numerical calculations with the fast field code, SAFARI [35] which incorporates shear effects. Additional calculations were performed with range dependent code which do not consider shear [36-38].

A feature of the shallow water experiments referenced here is the agreement with modal theory. Sound transmission loss results have agreed with modal theory insofar as the level versus range [3,6,14,18,20,21,22], interference patterns [3,6,11,20,22,21], the measurement of mode shapes [3,7,11,12,14,18,20], modal attenuation coefficients [5,13] and the horizontal wavenumber spectrum[21,22]. In addition measurements of the group velocity dispersion curve have been shown to agree with expectations[3,7,8,18]. These measure -ments have been performed in a variety of channels with several different bottoms. Although the results are quite different in many respects there is a remarkable consistency with the modal descriptions. Williams[39] has observed that since the profiles in the water column vary by only a few percent one would expect the qualitative understanding of the Pekeris wave guide to be robust. This observation must be taken with the understanding that a downward refracting profile emphasizes the bottom boundary condition and its dissipative effect. Here we investigate how well we can predict the measurements in a wave guide with a slightly downward refracting profile and independently measured geophysical and inferred geoacoustic parameters. This paper address the primary measurements while the work of our colleagues at the University of Miami [40] and the Rensselaer Polytechnic Institute [41] discuss the geoacoustic modeling and the inherent uncertainties in such models and the consequent variability in transmission predictions.

A interesting approach to the shallow water inversion or survey problem is the work of Frisk [21] and Lynch [22]. They used quadrature schemes and a synthetic aperture approach to perform the spatial Hankel transform to determine the Green's function kernel versus horizontal wavenumber [42] which we refer to as the horizontal wave number spectrum. We follow their lead and implement the synthetic aperture processing of Yen and Carey [43] which used a sequential series of Fourier transforms to produce the horizontal wavenumber spectrum for each hydrophone in the vertical array. This type of processing was accomplished at survey speeds and allowed the determination of the mode shapes from the depth variation of the wavenumber peaks. The comparison with numerical codes was

also facilitated by comparing the prediction of the magnitude and wavenumber of the spectral peaks. The experimental method presented here is an extension of the Frisk and Lynch work. First we describe the experiment and then we discuss the results in terms of the numerical calculations based measured environmental parameters.

2. Description of the Experiment

This experiment was conducted on the New Jersey continental shelf in the vicinity of a borehole (Amcor 6010) and near the Hudson Canyon. The general location and the bathymetric contours for this area are shown in fig.1. This particular area has been the subject of several ONR sponsored surveys. Shown in fig. 2 are the experimental transmission tracks (TL2-2,3-1,3-3) superimposed on the geopulse and Huntec survey tracks conducted by the Austin et al (1990). The constant engine speed tracks were parallel to the shelf (TL2-2/3-1) and perpendicular to the shelf (TL3-3) between selected way points:

Track	Way Point 1	Way Point 2
TL2-2	39° 01.2'N,73°08.0'W	39°04.3'N, 73° 04.9'W
TL3-1	39° 02.75'N,73° 06.5'W	39° 05.1'N, 73° 04.1'W
TL3-3	39° 02.75'N,73° 06.5'W	39° 11.8'N, 73° 21.9'W.

The basic experiment was to measure calibrated sound transmission for the cases of a constant depth and variable depth channels under calm sea state conditions and known environmental conditions. The basic parameters are shown in figure 3. the constant depth case was in 73 m of water while the variable depth case ranged from 73 m to 52 m depth. A continuous source of sound was used to produce four tones at time in sequences of 50-175-375-425 Hz and 75-275-525-600 Hz at source depths of 36 and 50 m.

2.1 The Measurement Systems

The sound source was a Naval Research Laboratory, Underwater Sound Reference Detachment (USRD) type J15-3, consisting of three moving -coil-driven rubber diaphragms. This transducer operated with source level of 165 dB re 1 μPa@1m at frequencies between 50 and 600 Hz. (Transmit current response was 164 dB//(1 μPa/1A@1m) and voltage 123 dB//(1 μPa/1v@1m) for a frequency of 50 Hz..) This source was mounted in a frame with a fin stabilizer which allowed tows of speeds to 7 knots. A depth gauge, known cable scope, and ship's speed enabled the determination of source depth by computation and measurement. A calibrated hydrophone (USRD-H91) was attached to the source with a 2 m flexible cable and was used to monitor the source level. The drive system for this source was referenced to a precision Ostron oscillator. This oscillator provided a stable reference signal to a programmable frequency synthesizer; the signal from this oscillator was conditioned, amplified and used to drive the Elgar power amplifiers. The drive amplifier voltage, current, and frequencies were monitored and recorded on a fourteen channel analog IRIG tape recorder along with the calibrated monitoring hydrophone and time code signal. Both the J15-3 and H91 were calibrated prior to the experiment at Dodge Pond to ensure the integrity of the USRD calibrations.. A dynamic spectrum analyzer was used during the experiment to monitor the calibrated levels from the H91 at the specific drive frequencies.

Figure 4 shows the vertical array and recording system used in this experiment. The system consisted of a sparbuoy (12 m (40 ft), 4.9 m (16 ft) above the surface) with a radar transponder, a 7.62 m (25 ft) tether, a subsurface buoy (700 lbs of buoyancy), a pressure

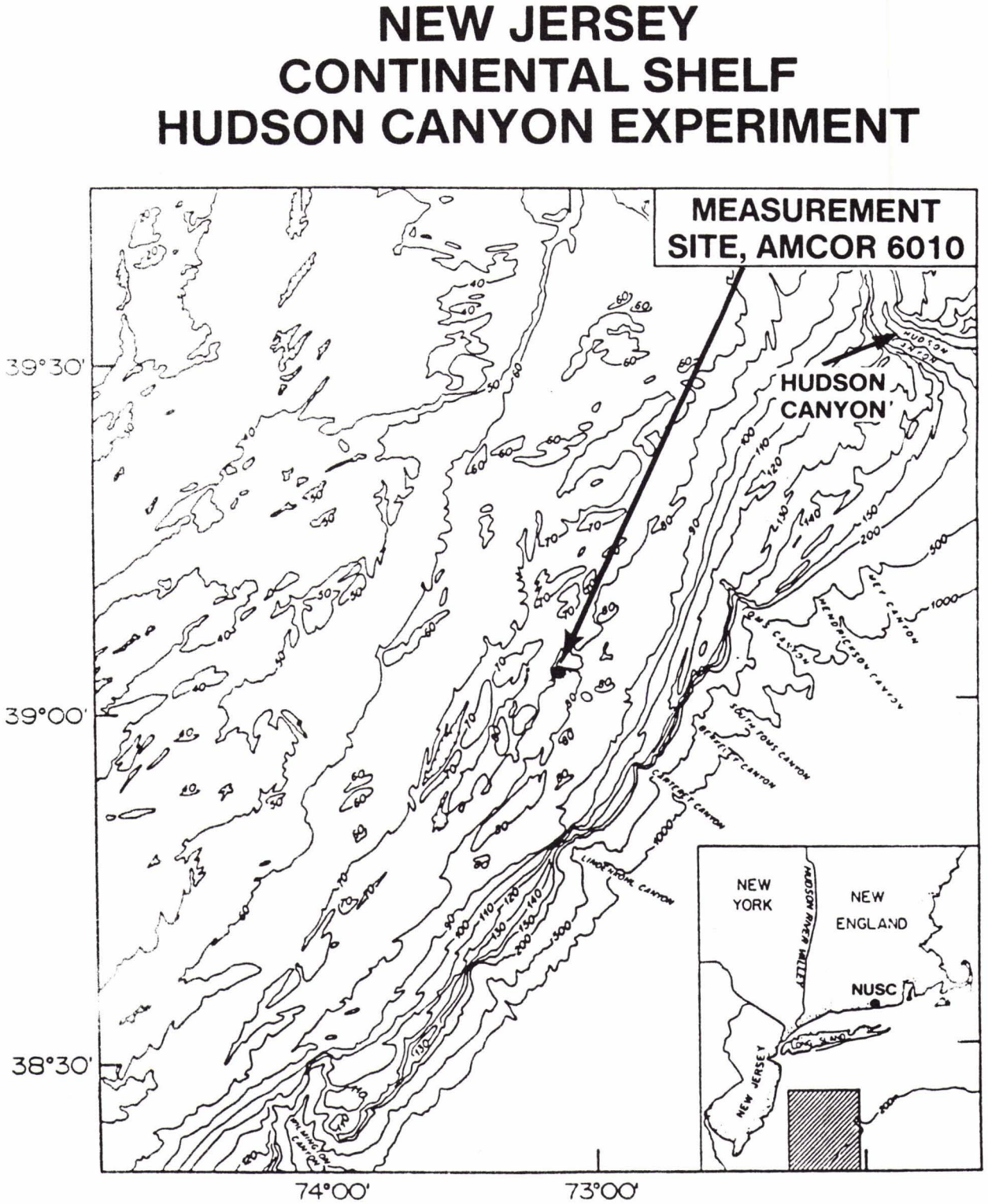

Figure 1. The experimental area and bathymetric contours are shown for the New Jersey shelf.

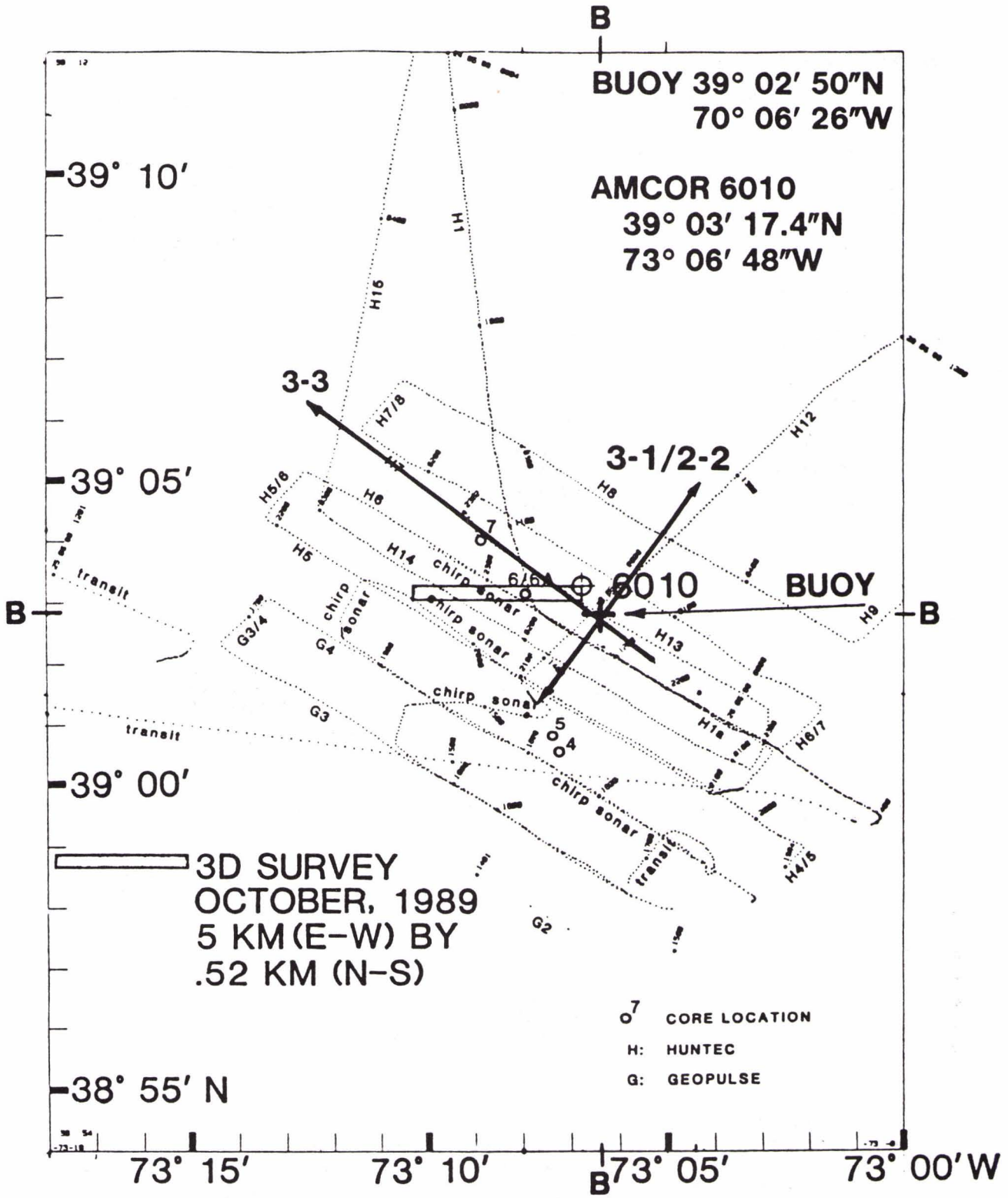

Figure 2. The experimental tracks for each transmission loss run are shown superimposed on the tracks of the Huntec 3-D survey of Austin et al [29].

- **TWO BASIC CASES:**

'A' UNIFORM DEPTH

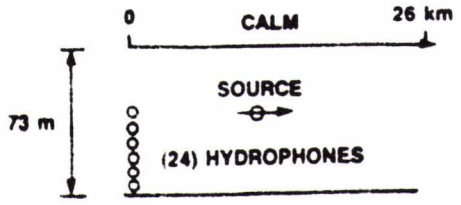

'B' VARYING DEPTH

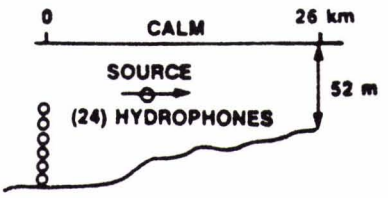

- **EXPERIMENTAL PARAMETERS**

WATER DEPTH:	'A' 73 m, 'B' 73 m → 52 m
RANGES:	0-4 km, 0-26 km
SEA STATE:	< BEAUFORT 2
OCEANOGRAPHIC COND.:	STABLE APPEARANCE, VARIABLE SVP
FREQUENCIES:	50-75-175-275-375-525-600 Hz
SOURCE DEPTH:	36 AND 50 m
SPEED:	CONTS. MIN. RPM (2 AND 5 kts)
RECEIVER DEPTHS:	24 CHANNELS- SPACED 2.5 m- "UP FROM BOTTOM"

Figure 3. The experimental parameters are shown for the flat and sloping bottom runs.

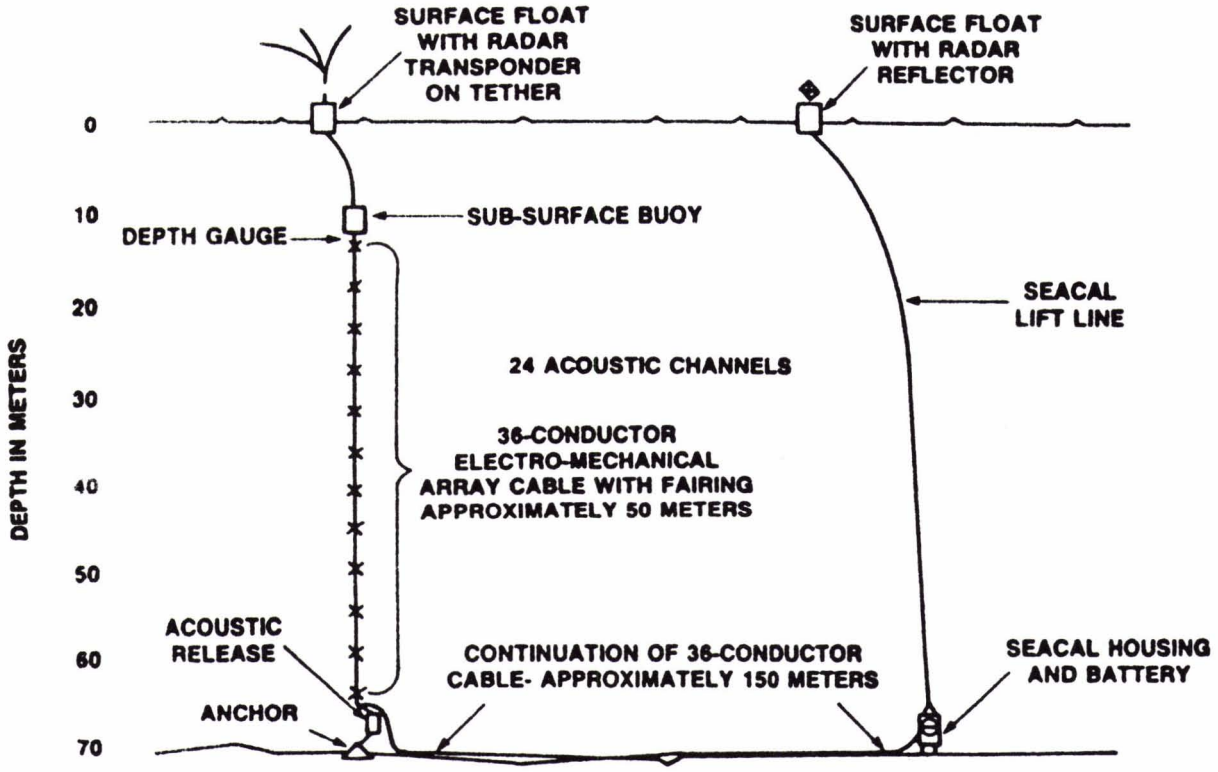

Figure 4 The receiving array is shown with the recording buoy at the end of a tether. This enabled the periodic lifting of the buoy to change the batteries and tapes without moving the measurement array.

transducer, 24 (Benthos AQ-17) hydrophones mounted on a "hair" faired cable with 2.5 m spacing, an acoustic release and a 1800 lb anchor. The pressure vessel and the recording electronics were located 150 m from the anchor. A 3/8 inch double braided lift line to a surface float enabled the lifting of the recording system for rapid refurbishment and battery replacement without moving the measurement array.

Although the subsurface buoy had sufficient buoyancy force to keep the array vertical, the length of the system between the anchor and the spar buoy was 78 m compared to the 73 m water depth. This resulted in a range bias of between 5-11 meters due to the drift of the sparbuoy and radar transdponder. The relative uncertainty in range determined by the radar transponder was determined by at sea and ashore calibrations to be ±2 m.

The experiment was designed to be conducted at constant ship speed. Two basic runs were conducted. The slower speed (1.835 m/sec) run shown in fig. 5 was conducted by selecting remote locations, referred to as "way points", at opposite extremes of the track with the buoy as the marker for the closest point of approach (CPA). This enabled a true course to be maintained. The speed was controlled by running the ship's power plant at a constant number of revolutions per minute, RPM. This slower speed also required the use of a single propeller and clutching on a set schedule. The longer range and higher speed tracks were performed with a single propeller and constant RPM operations. Due to the low sea states, lack of a strong prevailing wind and currents, we were able to maintain a fairly steady course , speed and CPAs of approximately 100 m. This is clearly shown in fig. 5 where we have plotted radar transponder range versus the elapsed time from the beginning of transmission loss run TL2-2. Since the depth averaged sound speed is 1497 m/sec, the expected Doppler shift is $\pm 1.23 \times 10^{-3} f_0$ or $\pm 6.14 \times 10^{-2}$ Hz for 50 Hz and $\pm 9.02 \times 10^{-2} f_0$ at 75 Hz.

The recording system was a 27 channel system which utilized two standard VHS tape recorders with a capacity of 10 gigabytes in either a standard record of 8 hours or a slow recording mode of 16 hours. Data was acquired from the 24 AQ-17-hydrophone channels, a depth gauge, and a reference clock. Each hydrophone channel had it's own signal conditioning consisting of a preamplifier, a 0 dB gain buffer amplifier, pre-emphasis (-6 dB/octave from 1kHz), a variable gain amplifier (0-48, 50-98 dB in 6 dB steps), an 8-pole Tchebychev anti-aliasing filter, and a sample-and-hold circuit followed by a 14-bit analog to digital converter (AID) with a 3263.4 Hz sample rate. All channels are sampled simultaneously preserving channel-to-channel information. Each channel's data sample is enabled on the data bus in sequence resulting in a bus data rate of 88,112 Hz digital words containing the depth, time code, and synchronization data were interleaved with acoustic data in a fixed repeating sequence. The AQ-17 hydrophones were chosen for their flat response between 10 Hz to 1 kHz. The mean hydrophone sensitivity was determined during the pretest calibration to be -174.3 dB re 1V/μPa ± 0.4 dB.

2.2 The Geo-acoustic Structure

The results of the Huntec survey by Austin et al [29] are shown in fig. 6. This computer enhanced two dimensional picture of the bottom is consistent with the geo-technical data of Hathaway et al (1976, 1979) from the AMCOR borehole number 6010. The striking features of this figure are the near surface layering, the "S" reflector, channels and the "R" reflector. This picture simply shows the first twenty five meters of the sandy- silty- clay layer. One must keep in mind that these structures are not those associated with the basalt layering which at this site is some 200 m below the water sediment interface. These near surface structures were formed by the raising and lowering of the sea level in the last 40 k years before present (BP) [29,30].

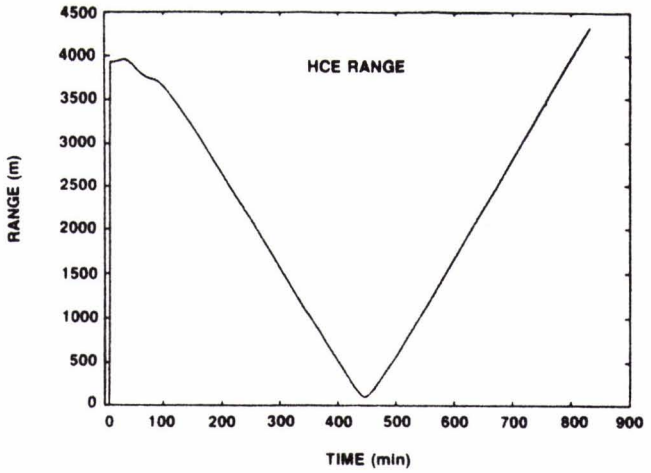

Figure 5. The relative range versus time for run Tl2-2.1, approaching the CPA, and run TL 2-2.2, distancing from the CPA.

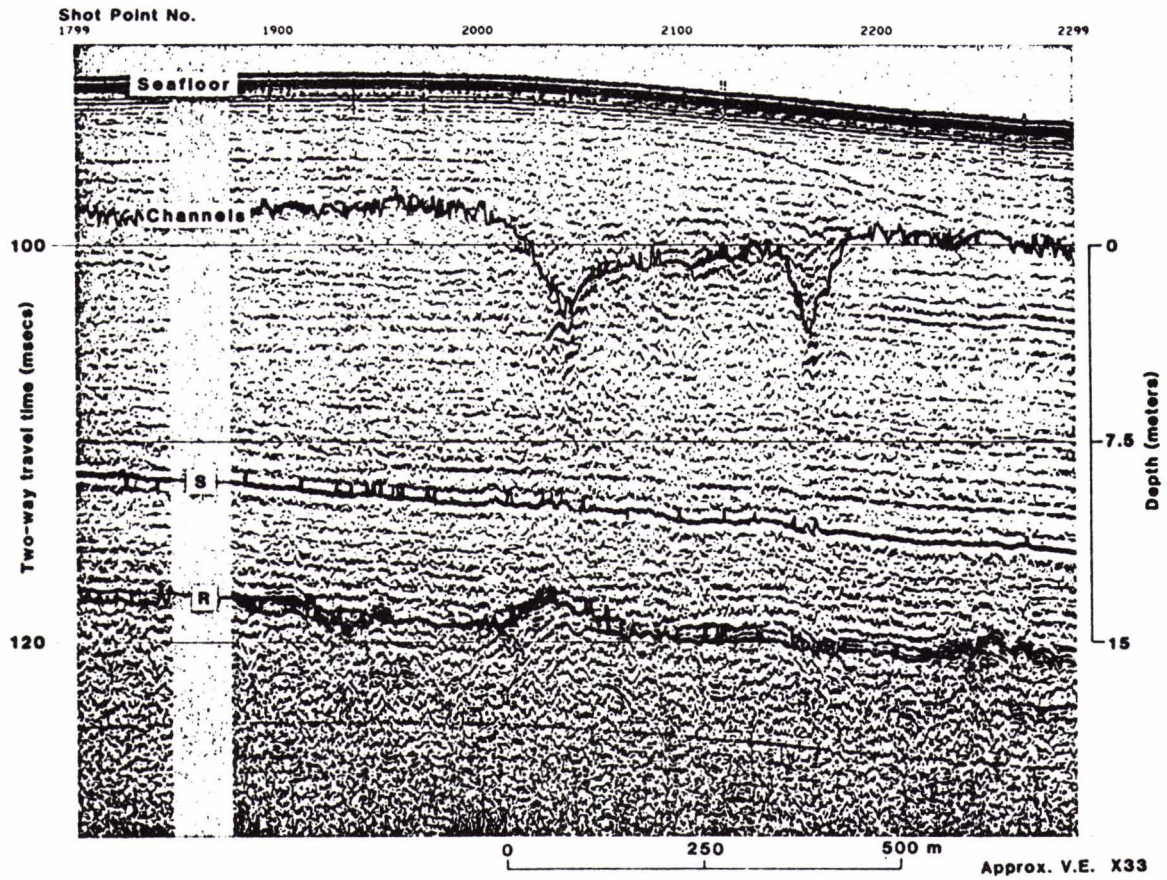

Figure 6. The near sediment structure from Austin et al [29] for the 25 m showing the near surface layering, the "channels", "S", and "R" reflectors.

In addition to the Huntec survey this area has been examined by Trevorrow and Yamamoto [32,33] and Stoll et al [31]. The Stoll group used a sledge excited by impulsive sources to excite shear waves . These shear waves were measured with an array of geophones. The detailed travel time curves and the small wavelength of the propagating shear waves permitted the least square estimation of the shear speed and attenuation versus depth . The Yamamoto group use the gravity-wave excited shear waves and an array to determine these same parameters. In this author's opinion the results from both authors are comparable. In this paper we use the estimates of these parameter as determined by Yamamotto and his research group. These values are tabulated in Table I and are used in the calculations of the sound transmission. The spread in the estimates of the near surface gradients and attenuation factors have been addressed by Cederberg et al [41] and are also summarized by Rogers et al [42].

2.3 The Measured Sound Velocity Structure

The conductivity, temperature and sound speed (SS) were measured as a function of depth with an Applied Microsystems Sound Velocity Profiler (SVP-16 referred here as SSP) and a SEABIRD Conductivity, Temperature and Depth (CTD) system. The simultaneous measurement of the SS and CTD profiles enabled a comparison of the directly measured

Table I. The geo-acoustic model

Depth (m)	Density (kg/m^3)	C_S (m/s)	C_P (m/s)	Q_P^{-1}	α_p (dB/λ)	Q_S^{-1}	α_s dB/λ)
5	1860	138	1.56	0.003	0.082	0.038	1.04
10	1960	182	1.61	0.0049	0.134	0.030	0.82
20	2090	260	1.74	0.0082	0.224	0.045	1.23
30	2170	326	1.83	0.0065	0.177	0.030	0.82
40	2090	310	1.76	0.0035	0.095	0.040	1.09
50	2030	299	1.71	0.0060	0.164	0.039	1.06
70	2050	331	1.74	0.0085	0.232	0.035	0.95
90	2180	436	1.91	0.0070	0.191	0.035	0.95
110	2240	504	2.01	0.0054	0.147	0.025	0.68
130	2210	501	1.98	0.0060	0.164	0.030	0.82
150	2170	487	1.94	0.0070	0.191	0.030	0.82
175	2100	450	1.85	0.0055	0.150	0.020	0.55
200	2090	455	1.85	0.0010	0.273	0.035	0.96

and the computed values using Wilson's equation. These measurements required the stopping of the research vessel and consequently SSPs were determined at the turning points of the transmission runs resulting in a two hour sampling at different locations. Figure 7 shows a representative set of temperature, salinity and sound speed profiles while fig. 8 shows several sound speed profiles all from the sound transmission run TL 2-2. The CTD computed and SSP curves are seen to compare favorably. The large differences observed in fig. 8 are due to the spatial and temporal variability of the sound speed structure. The sound speed profile (SSP) for time 1330 shows a near surface isospeed layer (C= 1522 m/s) extending to a depth of 19m followed by a decrease in sound speed with depth at a rate of $\partial C / \partial D = 3\ s^{-1}$ to a depth of 32 m and a layer with a mean speed of 1484 m/s. The SSP obtained at time 1630 has an isospeed layer (C=1518 m/s) extending to a depth of 12 m followed by a more gradual decrease in speed with depth of $\partial C / \partial D = 1.4\ s^{-1}$ to a depth of 35m where a layer with an average speed of 1488 m/s. The three sets of profiles shown in fig. 8 correspond to the beginning, CPA and end of run TL2-2 as shown in fig. 5. These variations in the profiles are representative of spatial and temporal variability observed during the experiment. Salinity variations, fig. 7, were also observed

in the region of decreasing temperature and sound speed and may indicate mixing or internal wave activity. The influence of these variations in sound speed structure have been examined by Cederberg et al [41] and shown to primarily effect the estimation of horizontal wavenumber from the type of synthetic aperture processing employed here.

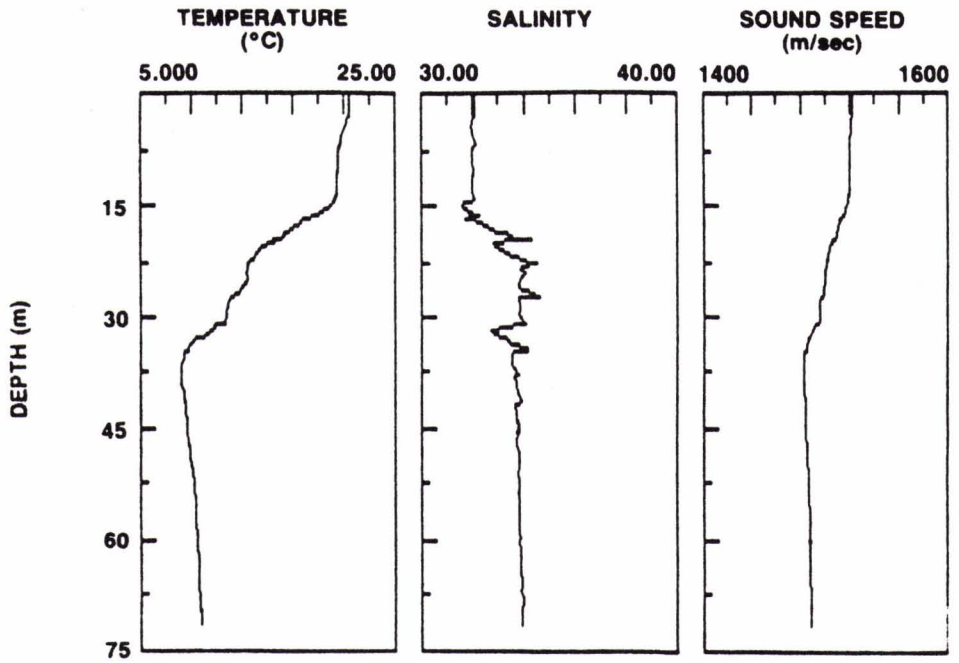

Figure 7. The measured temperature, salinity and sound speed profile for TL 2-2.

3. DISCUSSION OF THE EXPERIMENTAL RESULTS

This experiment consisted of the measurement of sound transmission over ranges 0-4 km and 0-26 km in a constant water depth and the over ranges 0-26 km in a variable water depth channel (73 m to 52 m). The 0-4 km sound transmission measurements were specifically conducted to determine the horizontal wavenumber spectra at survey speeds, while the longer runs were designed to measure propagation loss. However due to the calm sea states and controlled experimental conditions horizontal wave high resolution Doppler spectra were obtained for most runs.

3.1 Constant Water Depth Results

Transmission loss run TL 2-2 had three separate legs and two discrete frequency sets, reference fig. 3. Figure 9 (a,b) shows the transmission loss results for discrete frequencies of 50, 75, 175, 275, 375, 525 and 600 Hz. The first observation to be made concerns the striking modal interference pattern observed at the lowest frequencies of 50 and 75 Hz. These modal interference patterns persisted throughout our experiment. As the frequency is increased the interference pattern is not obvious, see the result at 175 Hz. At still higher frequencies another discernible pattern begins to become apparent as the range increases, for example see the result at 525 Hz. At the lower frequencies this interference pattern is attributed to the constructive interference between modes. However the patterns observed at the higher frequencies are consistent with the interference between up- and down- ray bundles which interact with the bottom at angles near the critical angle.

The measurements of pressure, range, and time enable the estimation of the horizontal wave number spectrum $P(k,\omega)$, by use of the previously discussed synthetic processing

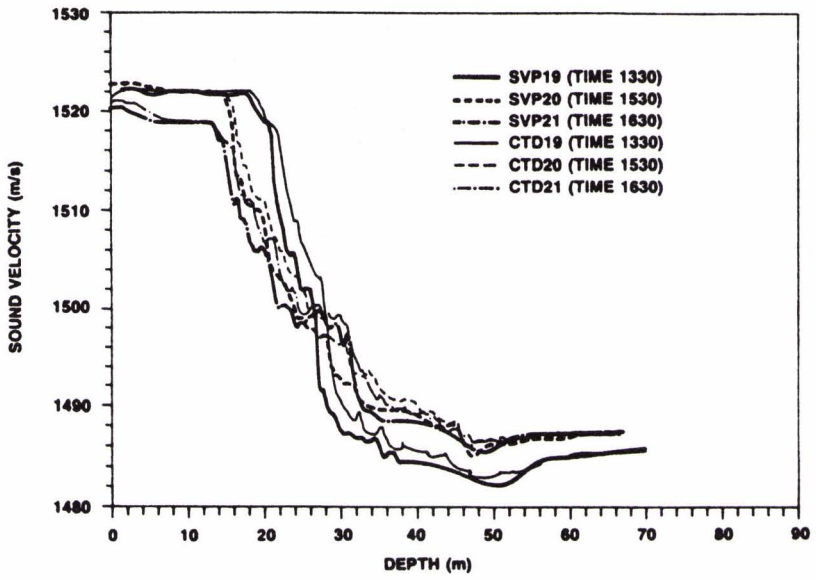

Figure 8. The measured sound speed profiles for fun TL 2-2 are shown for the begining , midpoint and end of the run. Also shown are the profiles derived from the measured salinity and temperature and Wilson's equation.

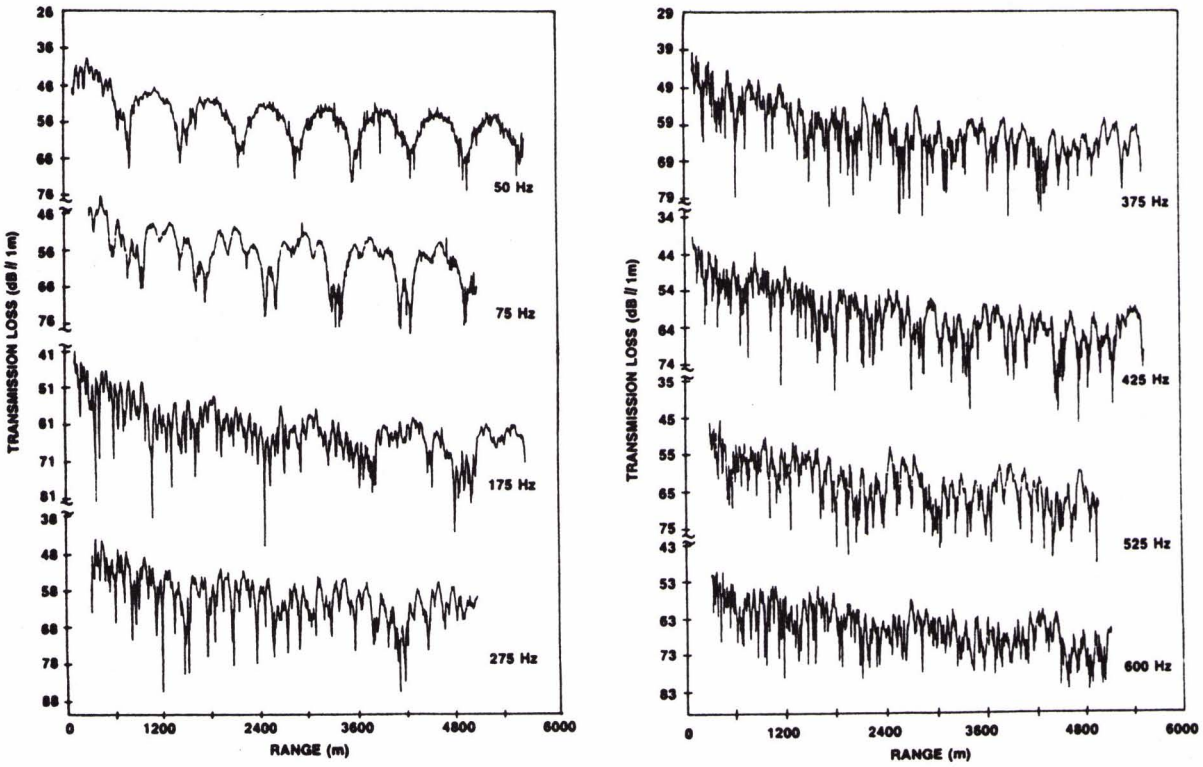

Figure 9. This figure shows the measured Transmission loss for runs Tl2-2.2and Tl2-2.3 corresponding to the previous sound speed profiles. Hydrophone 18 is at 57.45 m (188.5 ft) depth or 15.6 m above the bottom.

technique. Here we present the estimation of $P(k,\omega)$ determined by the sequential application of Fourier transforms and the subsequent application of a Hankel transform to the phase corrected sequence. If the pressure field $P(r,t)$ is sampled at some distance $r \pm \Delta r$ and time $t \pm \Delta t$, then the complex pressure, $P(r,\omega)$, is obtained first from the Fourier transform

$$P(r_n,\omega) = \int_{t_n - T/2}^{t_n + T/2} P(r_n,t) e^{-i\omega t} dt$$

$$= e^{-i\omega(t_n - T/2)} \int_{-T/2}^{+T/2} P(r_n, t_n, t) e^{-i\omega t} dt$$

$$= e^{-i\omega(t_n - T/2)} \sum_{m=1}^{M} P(r_n, t_n, mT/M)(T/M) e^{-i\omega mT/M}$$

and $$P(k,\omega) = \sum_{n=1}^{N} P(r_n,\omega) e^{ikr_n} \sqrt{r_n}\, \Delta r_n .$$

The quantity $|P(k,\omega)|$ versus ω is referred here as the wavenumber spectrum. Thus to determine $|P(k,\omega)|$, the accurate measurement of pressure, $P(r_n,t)$, range, r_n, and time, t_n are required. The measured estimate of $|P(k,\omega)|$ along with calculated spectra using the fast field program, Safari[34], are shown in fig. 10 for hydrophones 18 and 24 for a frequency of 50 Hz . The calculated values were based on a critical angle ($\approx 28^{o}$) bottom without shear corresponding to a step increase in density (2/1) and a sonic speed step from 1487 m/s in the water to 1560 m/s in the sediment. Calculations performed with Safari employing the geoacoustic profile of the previous section revealed that shear properties were not a factor in describing the propagation of sound at frequencies greater than 50 Hz. This is a result of the low values of the shear wave speed ($\approx$ 138-182 m/s, ref. Table I) characteristic of sandy-silty sediments found in many coastal areas. These shear wave speeds are comparable to the values used by Jensen and Kuperman [19]. The comparison between the calculated and measured spectra is good. The relative magnitudes of each mode agree but the wavenumber values are biased. This bias is due to uncompensated Doppler shifts, frequency mismatch and timing errors. We have shown that the measured wave number characteristic for the n^{th} mode is:

$$P_n(k,\omega) = P_{on}(k_n,\omega)\left|\sin(MVT(k - k_n + \Delta e)/2) / \sin(VT(k - k_n + \Delta e)/2)\right|$$

where M is the number of range samples, V is the constant relative speed, Δe is the error term, and $P_{on}(k_n,\omega)$ is the unbiased wavenumber function of the n^{th} mode. One can readily observe that this function has it's maximum value at $k = k_n - \Delta e$, a shifted wavenumber. In this instance the measured value of the horizontal wavenumber for the first mode at a frequency of 50 Hz was k=0.1987-0.1975 compared to calculated values of 0.2079-0.2080. Biased estimates of the actual wave number can always be expected in this type of processing when the measurements are performed at survey speeds. In this experiment another independent parameter was also measured, the effective mode shapes.

Figure 11 shows the relative magnitude of each measured horizontal wavenumber spectrum measured at a particular depth. Taken together these spectra allow the determination of the mode shape corresponding to each peak in the horizontal wavenumber spectrum. An interesting consequence of Snell's law is the invariance of the horizontal wavenumber for each mode. Furthermore we have the constraint that the square water wavenumber ($k_w^2(z)$) is equal to the sum of the squares of the horizontal (k_h^2) and vertical ($\beta_v^2(z)$) wave

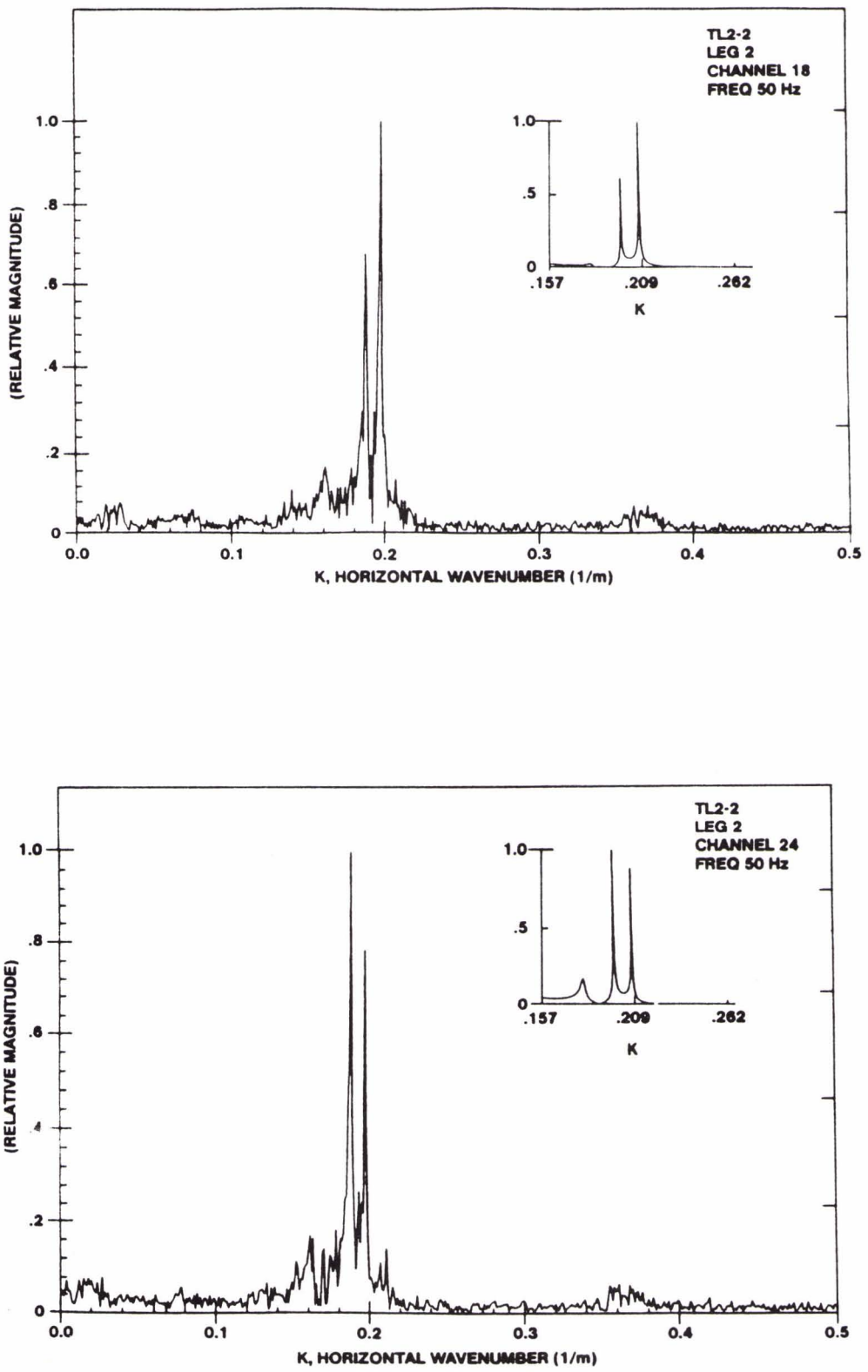

Figure 10. The horizontalwavenumber spectra are shown for hydrophones 18 and 24 for transmission run TL2-2. Also shown are the Safari calculated spectra for a two liquid layer environment.

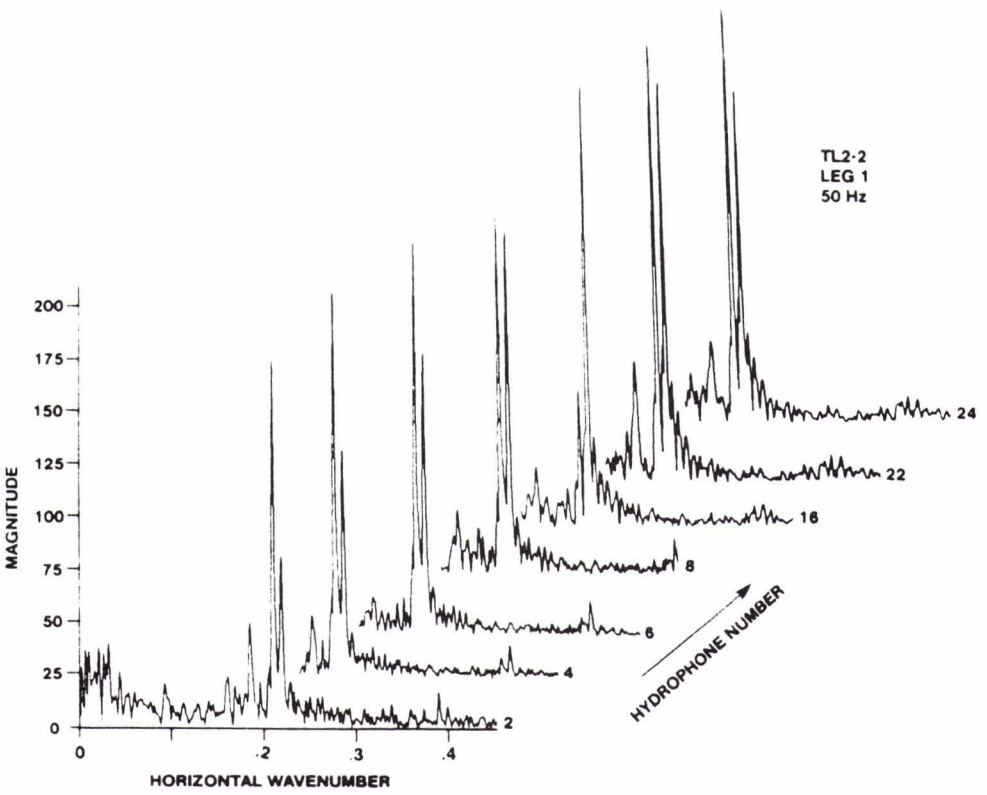

Figure 11. Shown here are the horizontal wave number spectra as a function of hydrophone number or depth along the vertical array. Hydrophone 24 is on the bottom and they are spaced at 2.5 m intervals.

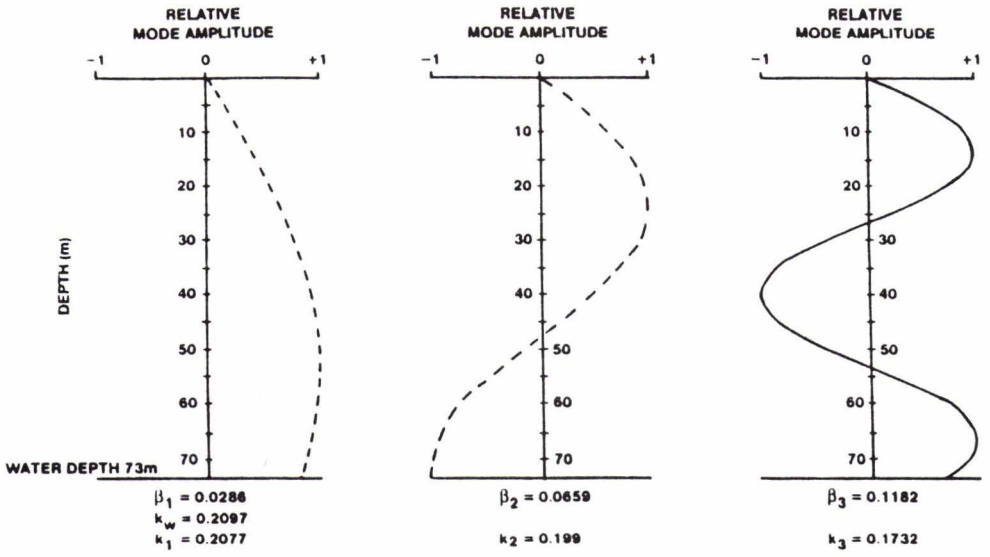

Figure 12. The mode shapes derived from the vertical variation of the horizontal wave number peaks. These shape represent the curve fits to the data.

numbers, $(k_w^2(z) = k_h^2 + \beta_v^2(z))$. Upon integration of this expression over the channel depth one finds:

$$k_h^2 = (1/H)\int_o^H k_w^2(z)dz - (1/H)\int_o^H \beta_v^2(z)dz.$$

This equivalent to the statement that the square of the horizontal wavenumber is equivalent to the difference of the mean square values of the water and vertical wavenumbers. In the case where the mean square is approximately the square of the mean one can consider the use of a mean vertical and water wavenumber and consequently remove the bias in the estimate of horizontal wavenumber. Shown in figure 12 are the modes at 50 Hz and 75 Hz obtained from the variation of the modal peaks with depth. The 50 Hz results were fitted by both a VLMS (visual least mean square) and a simplex (Nelder-Meade) algorithm. The horizontal wavenumbers were then adjusted to minimize the errors of the fit subject to the above constraint on the horizontal wavenumber, $(k_w^2(z) = k_h^2 + \beta_v^2(z))$. These estimates were obtained with the requirement that the surface is a pressure release one. Better fits may be obtained but do not satisfy this boundary condition which is appropriate for sea states 0-1. The results presented in Table II are consistent for two independent legs of the experiment, one inward towards the buoy and the other outward away from the buoy corresponding to the cases of up- and down-Doppler shifts.

Table II : Vertical and Horizontal Wavenumber Estimates

mode	1	2	3
f=50 Hz, k_w=0.2098			
$\beta_v(VLMS)$	0.0286	0.0659	0.1182
$\beta_v(simplex)$	0.0290	0.0662	0.1201
$k_h(LMS)$	0.2077	0.1990	0.1732
	0.2076	0.1990	0.1719
f=75 Hz, k_w=0.3147			
$\beta_v(VLMS)$	0.0330	0.0660	0.1346
$k_h(LMS)$	0.3130	0.3070	0.2840
f=75 Hz, k_w=0.3147, High Resolution Doppler Estimates			
β_v	0.0433	0.0806	0.1220
k_h	0.3120	0.3040	0.2899

Also shown in Table II are the results for 75 Hz. Two methods were employed to obtain the estimates of k_h ; the synthetic aperture method and a high resolution estimate of each mode's Doppler shift. This method simply requires a constant relative velocity and knowledge of the source frequency, i.e. $k_{on} = |(\omega_{dn} - \omega_o)/V|$.. The Fourier-Hankel transform pair for the nth mode may be written as:

$$P_n(k,\omega) = \int_o^R e^{ik_n r}\sqrt{r}\int_o^T P(r,t)e^{-i\omega t}dtdr\ ,\ R = MTV$$

and when r=Vt and $k_n = \omega\cos(\theta_n)/c$,it follows that

$$P_n(\omega) = \int_0^{MVT} P(V,t)(\sqrt{Vt})\, e^{-i\omega t} dt$$

This equation is recognized as the Fourier transform of the pressure multiplied by the spatial weighting factor ($\sqrt{Vt}$). This factor can be thought of as a shading term which will affect the width and relative magnitude of the spectral peaks but not the location as a function of Doppler shifted frequency and consequently horizontal wavenumber. Ignoring this factor simply yields for the nth mode: $\omega_{dn} = \omega_o\left(1 \pm V\cos(\theta_n)/c\right)$. The results shown in Table II were obtained with a 1200 sec FFT with a rectangular window .This is equivalent two a 2 km spatial transform. It is interesting to observe that both methods yield comparable results. However each method requires that different independent variables be known ; consequently the ease of measurement each approach is quite different.

Calculations were performed with the simulated critical angle boundary condition of a step increase in density by a factor of 2 and a step increase in sound speed from 1487 to 1560 m/s as well as the geo-acoustic profiles listed in Table I. The comparisons on the estimates of horizontal wavenumber are shown in Table III where the Safari results are for the simulated boundary condition while the Rogers[40] and Snap[35] calculations were performed with the geoacoustic model. A comparison of both relative amplitudes and wavenumber estimates shows excellent agreement. The purpose of presenting this comparison is to comment on the potential for inversion, that is more than one set of boundary conditions may yield equivalent sound pressure fields.

Table III: Horizontal Wavenumber Comparison

	Safari	Rogers[40]	SNAP	Experimental
k_1	0.208	0.2079	0.2086	0.2077
k_2	0.1978	0.1980	0.1989	0.1990
k_3	0.1797	0.184	0.1824	0.1732

As previously mentioned calculations with the estimated shear wave speeds for this experimental location show shear was not a factor. The agreement shown above was repeated in this experiment for additional runs on different days and at 75 Hz. This comparison shows that knowledge of the horizontal wavenumber spectrum to the third significant digit is required. Variations in the oceanographic salinity, temperature and sound speed profiles as well as our uncertainty of the spatial homogeneity of the bottom places hard limits on the measurements and the ability of one to utilize these types of results in inversion routines. Cederberg et al [41] have performed a detailed analysis of the inherent uncertainties in these measurements and have shown that sediment sound speed uncertainties and range dependent variations can cause significant variations in the third significant digit of the calculated wavenumber. The experimental uncertainties are more difficult to estimate. From the biased estimates of wavenumber obtained from individual hydrophone horizontal wavenumber spectrum, the uncertainty was determined to be $\Delta k = \pm 0.004$. The high resolution Doppler estimates yield $\Delta k = \pm 0.004$ $(50Hz)$ and $\Delta k = \pm 0.012$ $(75Hz)$. We therefore take as the underlying uncertainties in our experimental values $\Delta k = \pm 0.005$.

Figure 13 (a,b) for the inbound and outbound legs at 50 Hz shows the intensity level of each mode as a function of depth and horizontal wavenumber. Superimposed on these plots are the mean horizontal wavenumber spectra averaged over all 24 hydrophones. Both the mean spectrum and gray scale plots for both the in- and outbound legs are similar for the

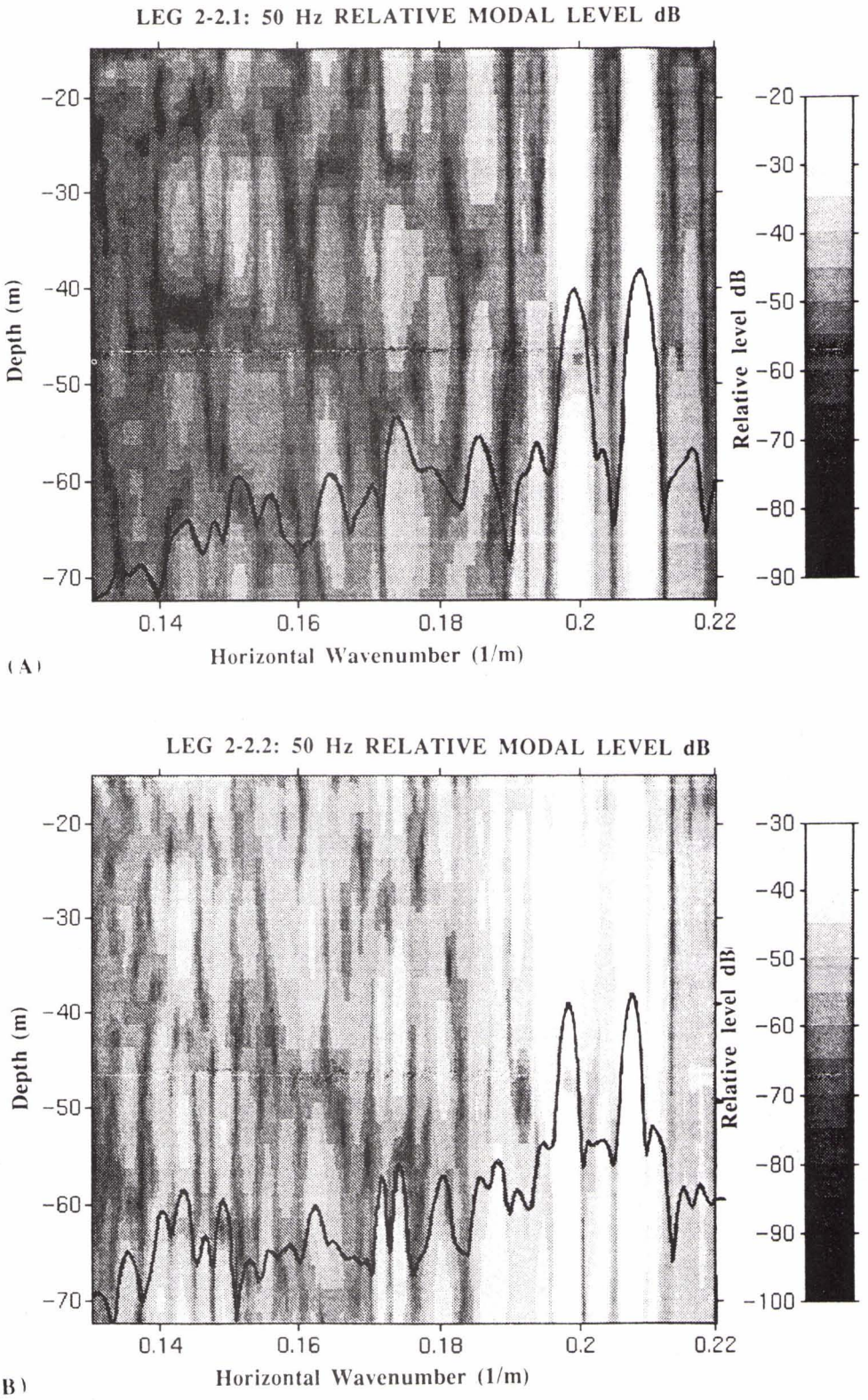

Figure 13. This figure shows shade plots of the modal intensity versus depth for the frequency of 50 Hz for a) TL2-2.1 and b) TL2-2.2. The sumperimposed line spectrum represents the vertically average horizontal wavenumber spectrum.

first two modes. Differences between the wavenumbers are 0.0009 for mode one and 0.0005 for mode two. As the wavenumbers become smaller more variability is observed. For example consider the wavenumber peak at k=0.1742 (TL 2-2.1) and the corresponding peaks at k=0.1742 and 0.1719 (TL 2-2.2). Examination of the range versus time curve for TL2-2 shows a constant range rate; consequently this effect of two similar modal wavenumber peaks is most likely not due to Doppler. This repetitive nature, that is the same number of maxima and minima with depth, of the two modal peaks in TL 2-2.2 is similar to the results obtained at 75 Hz.

The results for TL 2-2.3 Are shown in fig. 14 for 75 Hz. The spectral curve is the mean wavenumber spectrum of all 24 hydrophones. The wavenumber peaks at k=0.2731 and k=0.2842 have ghosts with similar repetitive patterns. These effects are not additional modes since the number of minima and maxima appear to be the same. Rather this repetitive nature may well be due to aberration caused by the range dependence of the sound speed structure within the water column. These effects are most important for TL 2-2.2 and TL 2-2.3 and. donot appear to be important for TL 2-2.1. This interesting insofar that TL 2-2.2 and TL 2-23 are over the same range dependent track. These speculative comments stress the variability in the measurement of the horizontal wavenumber spectrum and the need to consider this variability when inversions are performed.

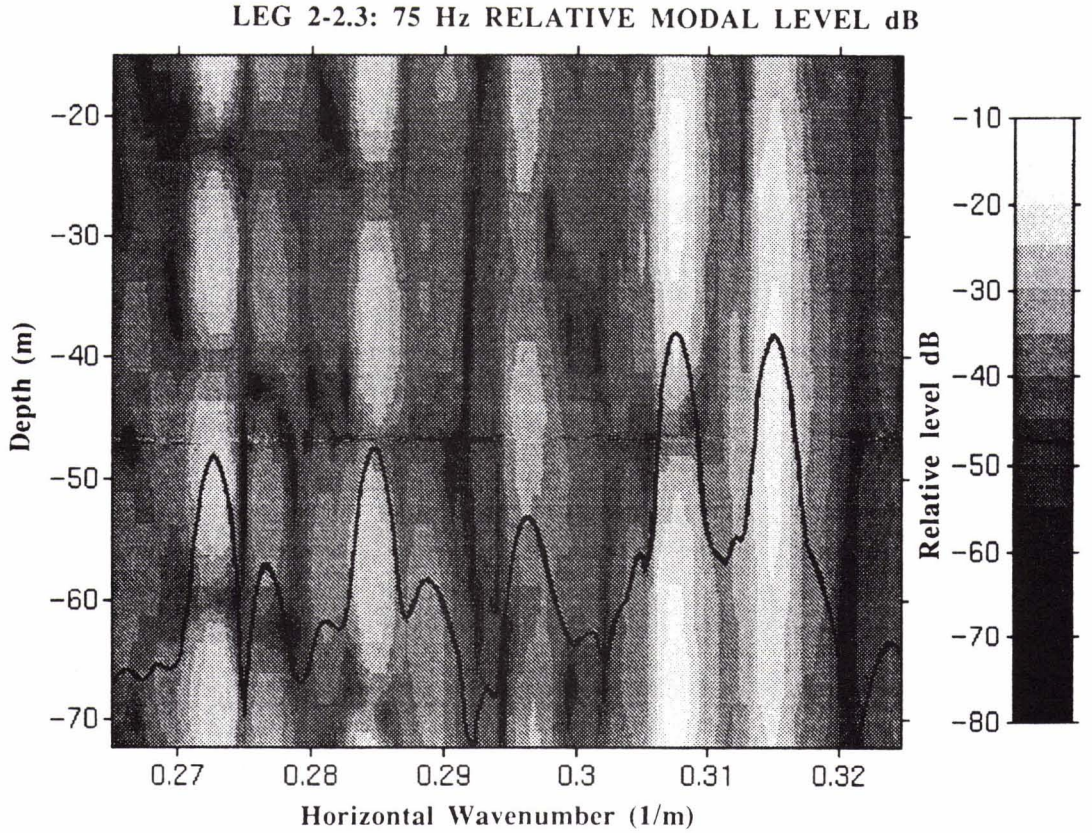

Figure 14. This figure show a shade plot of the relative modal intensity versus depth for the frequency of 75 run TL2-2.3. Also shown is the vertically averaged spectrum.

3.2 Range Dependent Results

Sound transmission was measured to ranges between 20 and 26 km for both the cases of a constant water depth (referred to as the flat bottom) and a range dependent bathymetry (sloping bottom). The 50 Hz results are shown in fig. 15. The flat bottom transmission loss results has the modal interference pattern characteristic of this experiment. At the extreme range, the dark-grassy nature of the curve is due to the decrease in signal-to-noise ratio. The transmission loss curve for the sloping bottom case has two range dependent features. First observe the change in the modal interference pattern between 7 and 14 km. Second as the water depth decreases we see a slight enhancement (a decrease in transmission loss) and a unimodal structure; again, the grassy nature of the trace is due to the reduced signal to noise ratio. This change in the interference pattern was considered significant as on multiple days a repeatable interference pattern was consistently observed. Furthermore this change occurs with small change in water depth.

High resolution FFTs (1.2 mHz, corresponding to a 2km sample) were performed to examine the range dependence of the modal structure. The flat bottom cases for 50 Hz and 75 Hz revealed high-resolution-Doppler-shifted modal peaks with a repeatable structure. These results were presented in Table II and the horizontal wavenumbers estimates were comparable to those measured in test TL2-2 for the first two modes. However, these characteristic wavenumber spectra were not found in the range dependent case. Figure 16 shows 9 consecutive spectra for the upslope transmission run at 50 Hz. Each spectrum covers a range interval of approximately 2 km. Spectra 3 and 4 reveal an anomalous change in the spectral structure. That is, the wavenumber spectrum measured by a vertical array in 73 m of water from a source towed at a constant speed and depth over a gently sloping bottom results in a wavenumber spectrum different than from the deeper flat bottom case. These anomalous spectral features are not due to the speed of the ship or to drastic changes in the sound speed profiles. Rather these changes occur in the vicinity of changes in the sediment sub layering. The "R" reflecting layer, fig. 6, varies with range as one proceeds upslope at a faster rate than the water sediment interface. In the range interval between 7 and 12 km, this reflector produces a near surface layering which is variable and covered by a thin veneer of sand. This results in a rougher and stronger impedance contrast with a much higher shear wave speed.

This range dependent effect was modeled neglecting shear by allowing the S and R layers to rise to the surface at a distance of 10.25 km from the source. The properties for the calculation which was performed with the Finite Element Parabolic Equation FEPE code.

TABLE III

LAYER	$C_p(m/s)$	$C_s(m/s)$	$\rho(gm/cm^3)$	$\alpha(dB/\lambda)$
1	1560	138	1.86	0.082
2	1610	182	1.96	0.134
3	1847	326	2.13	0.183

At the 10 km range the top two layers was removed for a distance of 500 m . The water sediment interface was held at 73 m and the bottom of the second layer was at a depth of 93 m until a distance of 9.75 km at which point it shallows to 73 m at a distance of 10.25 km and then remains constant to range of 10.74 km. This type of impedance change produced a marked change in the modal interference pattern. This is similar to the experimental observation and indicates that sub-bottom layering can drastically affect the propagation of low frequency sound.

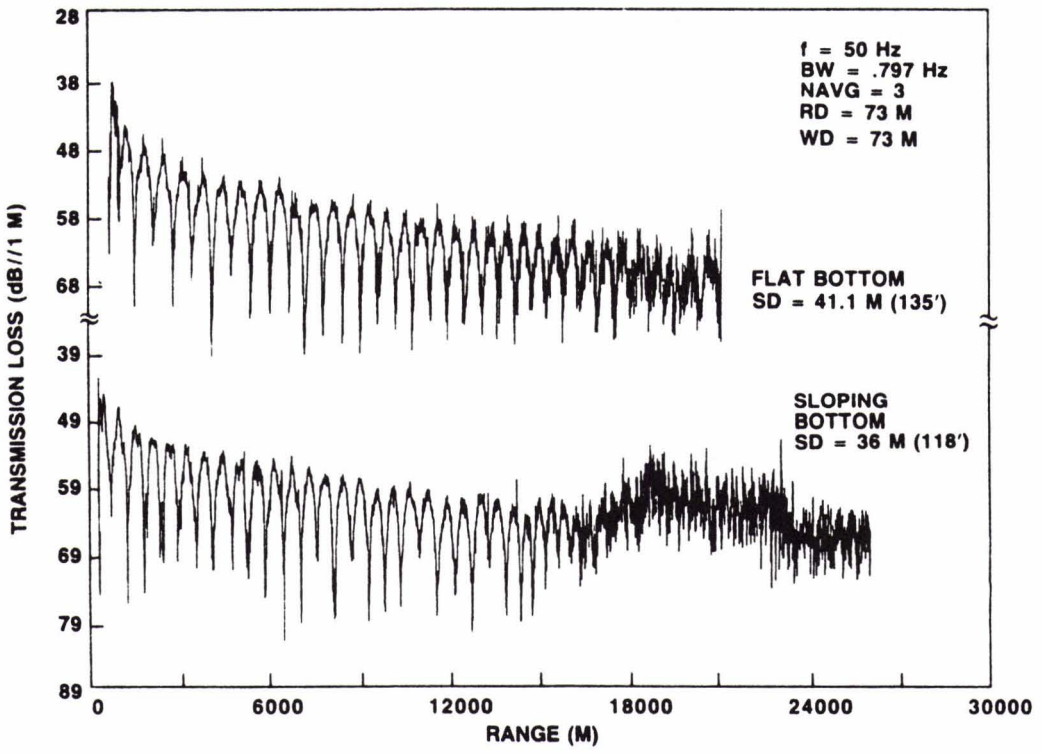

Figure 15. The transmission loss measured for the flat (TL3-1) and sloping bottom (TL3-3) runs shows the effect of the slope and a change in modal structure.

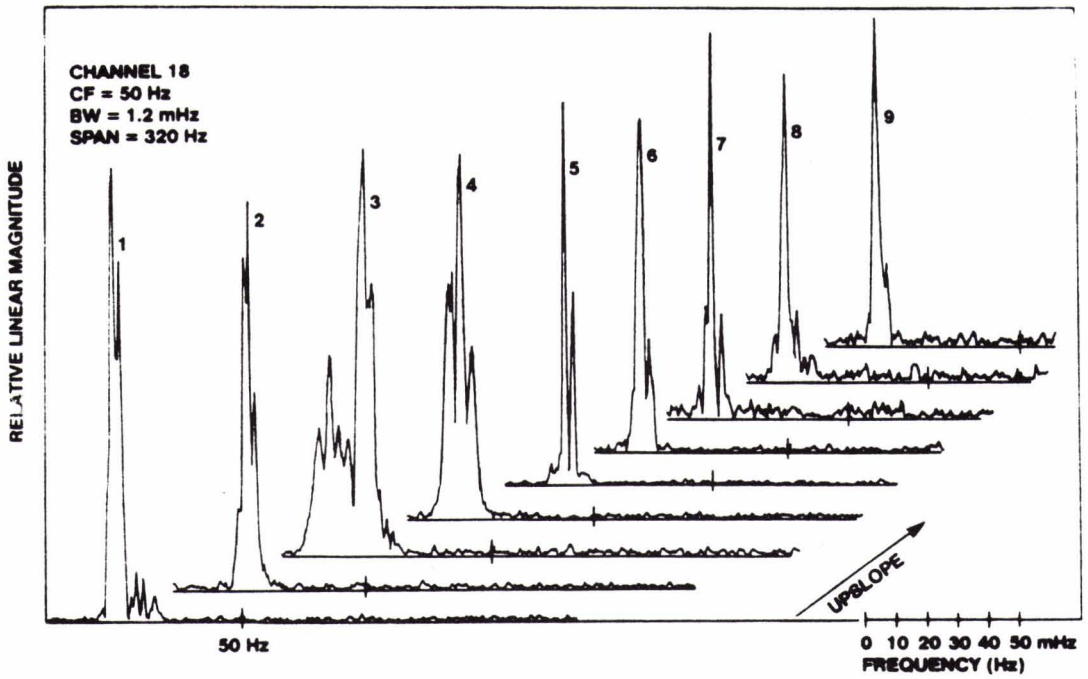

Figure 16. Shown here are consecutive high resolution Doppler shifted spectra. The peaks coresspond to individual modes with different Doppler shift. Spectra 3 and 4 show anomalous spectral peaks thought to be the result of a changing bottom.

3.4 Numerical Comparisons

Several codes were employed to numerically describe the sound transmission results. First Safari was used to determine the importance of shear effects. The geoacoustic parameters were those listed in Table I and the particular run was TL 2-2, the constant depth radial. Calculations with and without shear at 50 Hz were identical and as previously seen the data were described by simply treating the sediment as a liquid. The agreement between the measured and calculated sound transmission was in fact remarkable. Since shear effects were not important the range dependent radials could be treated with either IFD/PE or FEPE. The consistency of this approach was determined by requiring that each code yield comparable results. In general we found that Safari, Kracken [36], FEPE [38], and IFD/PE[37] yielded indistinguishable results for the range independent case.

Cederberg[41] performed calculations with the IFD/PE for the TL2-2 transmission run. A comparison of our simplified boundary condition, the geoacoustic model and a comparison with data are shown in fig. 17 for 50 Hz and in fig. 18 for 75 Hz. The 50 Hz result is comparable to the calculated wave number spectra shown previously for the two layer isospeed model. The solid dark curve is the transmission data(displaced by -15 dB), the dotted curve is the geoacoustic model (A) result, and the chain dotted curve is the isospeed model (displaced by +15 dB). The calculated transmission loss for the isospeed profile has a beat pattern which is simply due to the interference of the two dominant modes an is consistent with the experimental results (level and skip distance) at longer ranges. The depth dependent model (A) chosen for this calculation was based on the application of the Biot theory to the geophysical data obtained from the AMCOR 6010 borehole and is an approximately the same (within 10%) of the TABLE I values. This approach was chosen here to allow the variation of geophysical parameters as discussed by Cederberg (1993). The near sediment surface gradient was taken to be a decrease in sound speed by 75m/s in the first 5 meters. The result shows very good agreement with the data. This calculated result agrees with the measured level, the modal skip distance and the presence of the higher order (low wavenumber) modes which attenuate with range. However one will note that two radically different profiles described this 50 Hz transmission loss result. This result is also true for the 75 Hz result. Figure 18 shows the results for 75 Hz for two different models. The a model is the same as for fig. 17 while the model (B) changes several parameters such as water depth, sediment gradients, and the sound speed at the inflection points of the profile. The agreement with the measured relative intensity level is excellent. These variations in the sound speed profile are within the expected uncertainties of the measured values.

The longer range "flat bottom" run , TL 3-1, and " sloping bottom" run, TL 3-3 results are shown in figures 19 and 20. The experimental data (solid curve) is over plotted with the FEPE calculated transmission loss (dashed curve). The results are shown for 50,75,175 and 375 Hz for hydrophone 18; however results for other frequencies and hydrophones are similar. Again we find excellent agreement at the lower frequencies and increasing disagreement as the frequency is increased. The calculations with SAFARI showed the same effect. The data have more loss than is predicted by a significant amount. The sloping bottom run seems to produce levels in closer agreement at the frequency 375 Hz. The results (not shown here) at 600 Hz (Rogers[40]) were found to have significant differences. Since we have included realistic values of attenuation in the sediment, these effects are attributed to interfacial roughness near the water sediment interface. The roughness is partially accounted for in the variable bathymetry used for TL 3-3 and could explain the reduction in differences at 375 Hz but not as the frequency is further increased. Interfacial roughness and volume inhomogeneities in the first several meters such as shown in figure could explain this excess attenuation. Rogers [40] estimated the magnitude

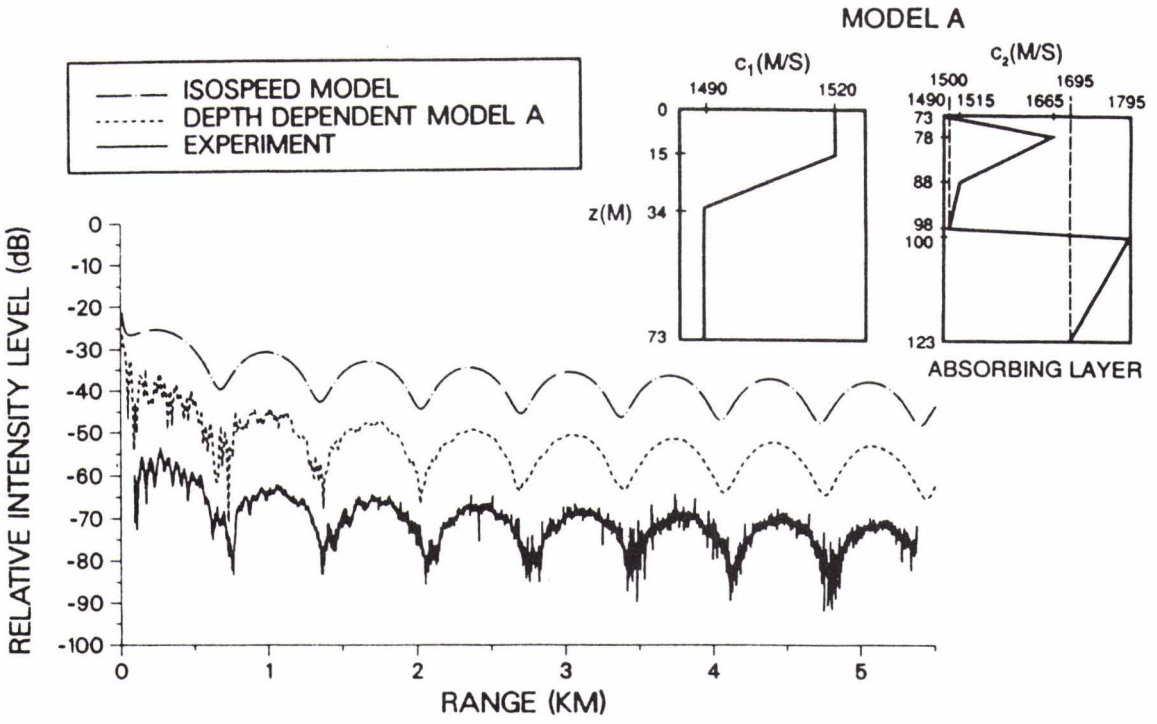

Figure 17. This figure compares the 50 Hz transmission loss results for run TL2-2 with calculations using IFD/PE and two bottom models.(Cederberg [41])

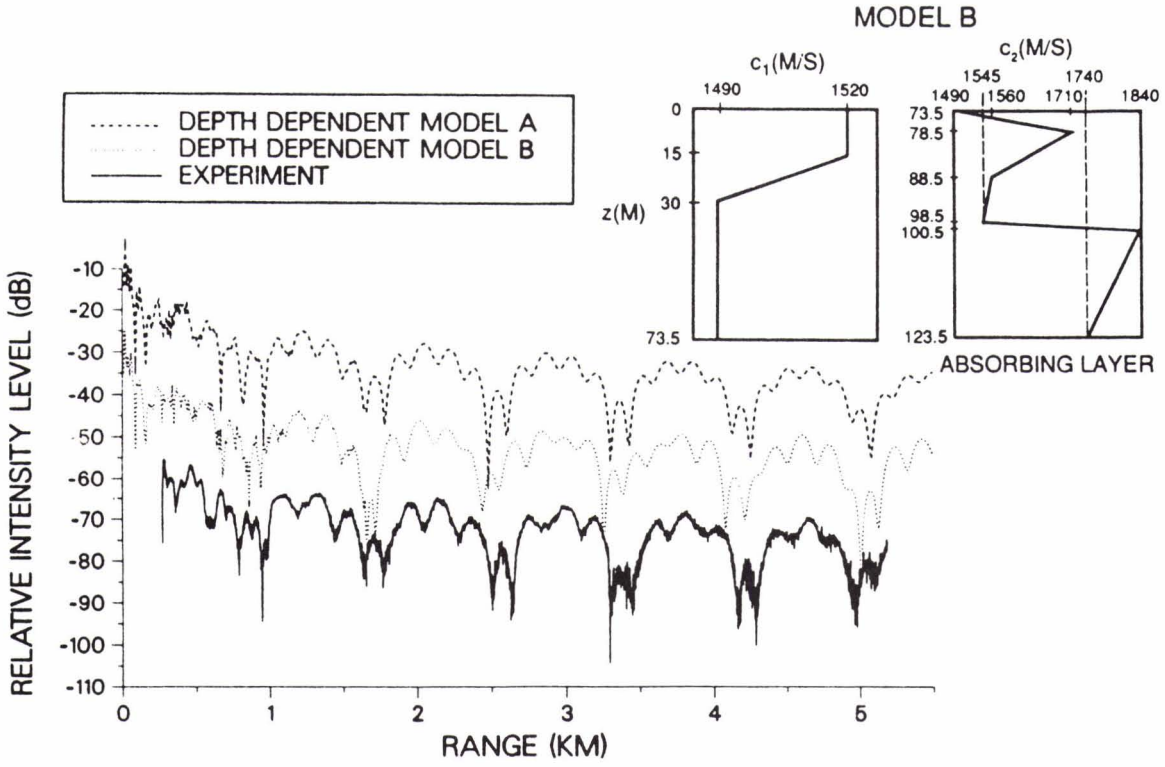

Figure 18. This figure shows a comparison with 75 Hz transmission loss results for run TL 2-2 and calculations performed with IFD/PE and Two bottom models.(Cederberg [41])

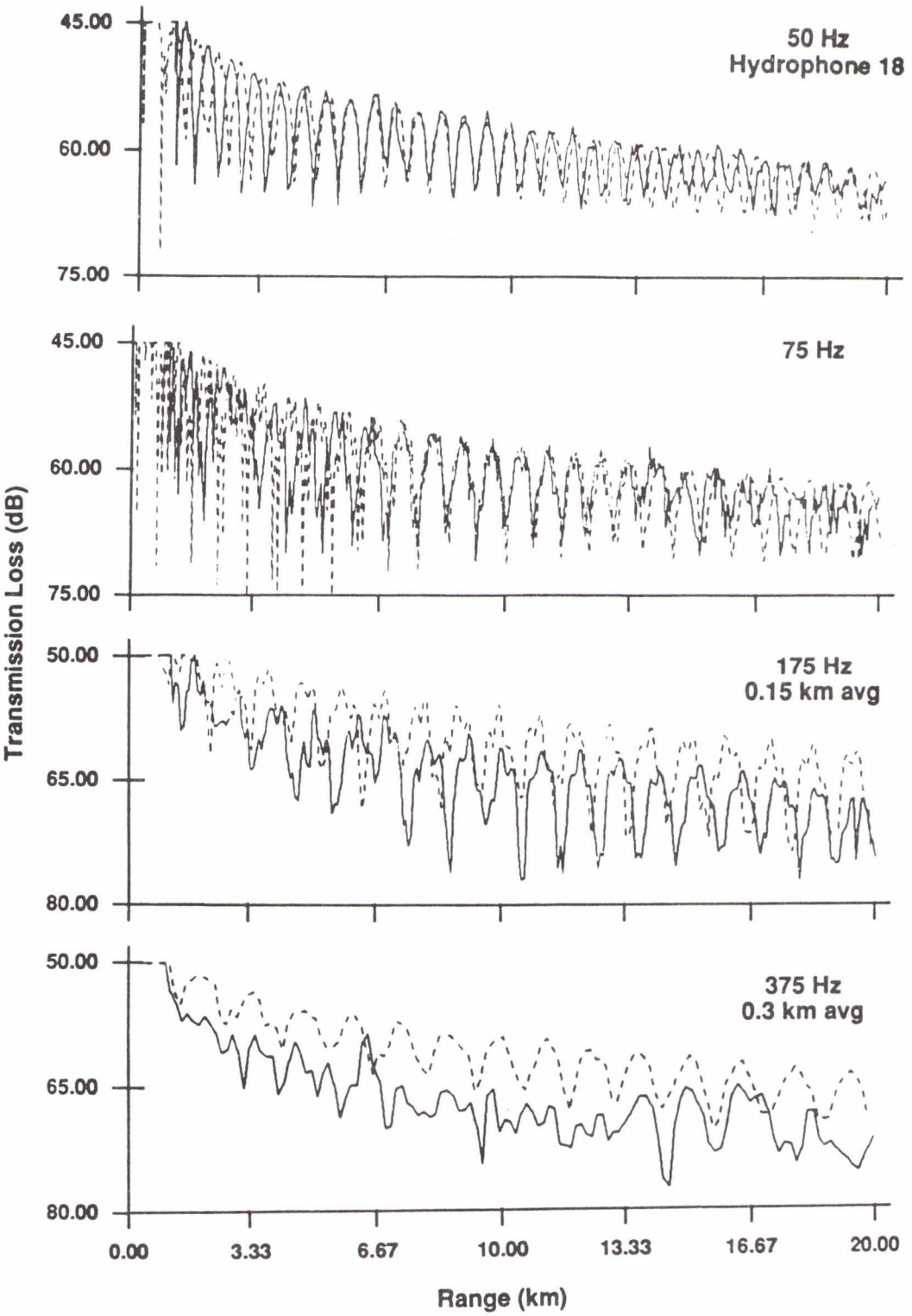

Figure 19. The transmission loss is shown for several frequencies for the flat bottom run TL 3-1. Also shown are the calculations performed with FEPE using the geoacoustic model

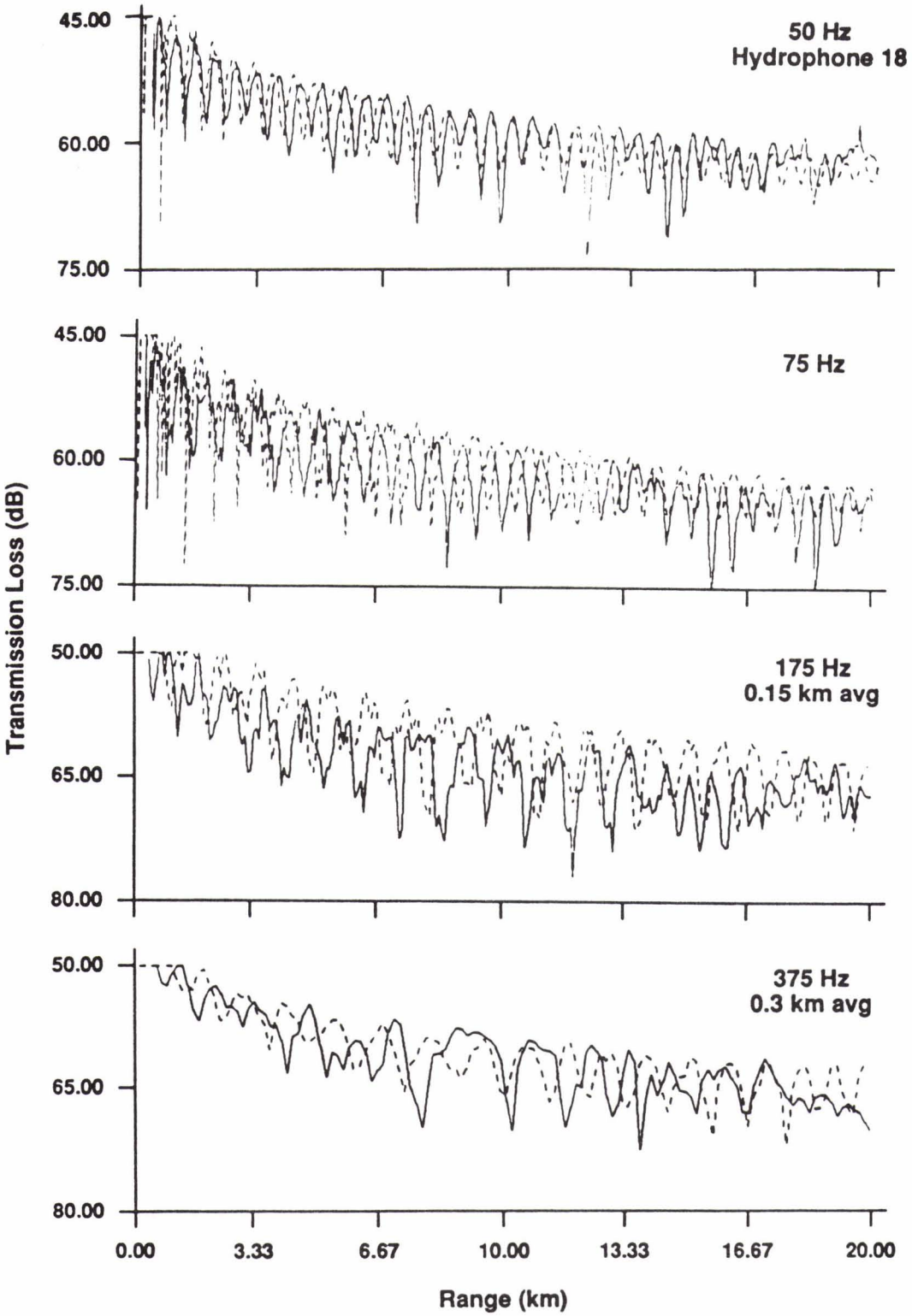

Figure 20. Transmission loss is shown for several frequencies for the sloping bottom run TL 3-3. Also shown are the calculations performed with FEPE, the geoacousti model and a range dependent bottom.

of these scattering effects and showed that the loss measured at the higher frequencies could be explained by this type of scattering.

4. Summary and Conclusions

We have discussed calibrated acoustic measurements obtained on the continental shelf of New Jersey. These measurements were taken over the period of a week in calm sea state conditions. The characteristics observed in this experiment were the repeatable modal interference patterns for both the flat and slopping bottom runs. The low frequency transmission loss results were found to be described by calculations using geo-acoustic profiles obtained from borehole data and Yamamotto's BSMP method with the first 30 m of sediment being the most important. It was also observed that a simple critical angle bottom also produced favorable comparisions for the first couple of modes. These results show that for the sandy -silty - clay sediments found in this experiment that shear effects were negligible at the lower frequencies. Thus the discrepancies between the measured transmission loss and the calculated values at the higher frequencies should not be attributed to shear but rather interfacial roughness of the bottom and sub-bottom layers or sediment volume inhomogeneities. We showed that bathymetric roughness has an effect and Rogers [40] has shown that scattering from the near surface sediment layering and volume could explain these losses. These results are consistent with the previous experiments and the observation of Williams[44].

A central theme of this experiment was to examine the synthetic aperture Hankel transform (Frisk and Lynch [22]) as a shallow water survey tool. We extended the method by performing the synthetic apertures at tow speeds of between 2 and 5 knots. The transform was performed using the sequential Fourier transform method (Yen and Carey[43]) and applying phase correction factors. In addition we used a high resolution Doppler technique to estimate horizontal wave numbers . These techniques, although difficult, worked very well for the flat bottom runs. The sloping runs showed that variable and anomalous results can be obtained. The horizontal wavenumber spectrum was found to be apparently influenced by range dependent features, most likely sub-bottom features representative of many coastal areas. If these techniques were to be used in inversions to obtain geoacoustic or bottom reflection coefficients , then these range dependent effects need to be considered. As shown here since the synthetic aperture processing can be accomplished by sequential Fourier transforms then the use of a horizontal array and subaperture processing is possible at survey speeds.

Comparisons with calculations performed with standard propagation codes verifies the importance of sub- bottom features such as the near surface layering, channels, S and R reflectors. These calculations also show that Williams (1976) was correct in his assessment with respect to the depth at which we need to know geoacoustic parameters. In this particular area 20 to 30m should suffice. Since subbottom feature are important in the forward sound transmission then they should be extremely important scatters. Finally we conclude that much work needs yet to be done to develop shallow water survey tools and techniques.

a) The Woods Hole Oceanographic Institution (WHOI), Woods Hole, Ma. 20543
b) Science Applications Incorporated (SAIC), New London, Ct. 06320
c) The Naval Undersea Warfare Center (NUWC) New London, Ct. 06320

5. References

[1] Urick, R. J. (1982): Sound Propagation In The Sea , (Peninsula Pub., Los Altos, Ca.)

[2] Eller, A. I., (1984): "Acoustics Of Shallow Water: A Status Report", NRL Rpt. 5405, (Naval Res. Lab. ,Wash.,D.C.-Avail DTIC).
[3] Pekeris, C.L., (1948):"Theory of propagation of explosive sound in shallow water", Geol. Soc. Am. Mem. 27, (The Pekeris theory is treated in: Elastic Waves In Layered Media, Ewing, Jardetzky, and Press, (McGraw Hill Book Company,Inc. New York,1957) and in: Introduction To Theory Of Sound Transmission, Officer, C.,B., (McGraw Hill Book Company Inc.,1958).
[4] Brekovskikh, L.M., (1960): Waves in Layered Media, Academic Press, New York.
[5] Kornhauser, E. T. and Raney, W.P., (1955):"Attenuation in shallow-water propagation due to an absorbing bottom", J. Acoust. Soc. Am. 27(4), 689-692.
[6] Tolsoy,I., (1958): "Shallow water test of the theory of layered wave guides", J. Acoust. Soc. Am. 30(4),348-361.
[7] Tolstoy, I., (1960): " Guided waves in afluid with continuously variable overlying an elastic solid: Theory and experiment", J. Acoust. Soc. Am. 32(1), 81-87.
[8] Barakos, P.A.,(1962):"Experimental determination of compressional velocity for the bottom layer by the dispersion method", J. Acoust. Soc. Am. 34(12), 1919-1926.
[9] Tolstoy,I. and Clay ,C.S. (1966): Ocean Acoustics, McGraw-Hill Book Co., New York.
[10] Bucker, H.P., (1964): "Normal-mode sound propagation in shallow water", J. Acoust. Soc. Am. 36, 251-258.
[11] Bucker, H. P., (1970): " Sound propagation in a channel with lossy boundaries ", J. Acoust. Soc. Am. 48(5 pt. 2),1187-1194.
[12] Ferris, R. H., (1972): "Comparison of measured and calculated normal mode amplitude functions for acoustic waves in shallow water", J. Acous. Soc. Am. 53(3pt2), 981-988.
[13] Ingenito, F., (1973): "Measurements of mode attenuation coefficients in shallow water", J. Acoust. Soc. Am. 53(3), 858-863.
[14] Ingenito, F. and Wolf, S. N., (1976): "Acoustic propagation in shallow water overlying a consolidated bottom", J. Acoust. Soc. Amer. 60(3), 611-617.
15] Cole, B. F. and Podeszwa, E. M., (1967): " Shallow water propagation under downward refraction conditions", J. Acoust. Soc. Am. 41(6), 1479-1484.
[16] Cole, B. F. and Podeszwa, E. M., (1974): "Shallow-water bottom rever-beration under downward refraction conditions", J. Acoust. Soc. Am. 56(2), 374-377.
[17] Cohen,J. S. and Cole , B. F. (1977): "Shallow water propagation under downward - refraction conditions. II", J. Acoust. Soc. Am. 61(1), 213- 217.
[18] Rubano , L.A. (1980): " Acoustic propagation in shallow water over a low velocity bottom", J. Acoust. Soc. Am. 67(5), 1608-1613.
[19] Jensen, F. B. and Kuperman, W.A., (1983): "Optimum frequency of propagation in shallow water environments", J. Acoust. Soc. Am. 73(3), 813-819.
[20] Jensen, F. B. (1981):" Sound propagation in shallow : a detailed description of the acoustic field close to the surface and bottom" J. Acoust. Soc. Am. 70(5), 1397-1406.
[21] Frisk, G. V. and Lynch, J. F. (1984): "Shallow water waveguide characterization using the Hankel transform", J. Acoust.Soc. Am. 76(1), 205-216.
[22] Lynch, J. F., Rajan, S.,D., and Frisk, G. V., (1991): " A comparison of broadband and narrow-band modal inversion for bottom geoacoustic properties at a site near Corpus Christi, Texas", J. Acoust. Soc. Am. 89(2), 648-665.
[23] Hathaway, J.C., Schlee,J.S., Poag, C.W., Valentine, P.C.,Weed, E.G.A., and Schultz, D.M., (1976): "Preliminary summary of the 1976 Atlantic margin coring project of the U.S. Geological Survey", U.S.G.S. (open file rept. 76-844).
[24] Hathaway, J .C., Poag, C.W., Valentine, P.C., Miller, R. E., Schultz, D. M., Manhiem, F. T., Kohout, F.A., Bothner, M.H., and Sangrey, D. A., (1979): " U.S. Geological Survey core drilling on the Atlantic Shelf," Science 206, 515-527.
[25] Biot, M. A.,(1956): " Theory of elastic waves in a fluid-saturated porous solid. I. Low frequency range", J. Acoust. Soc. Am. 28, 168-178.

[26] Hamilton, E. L., (1980) : "Geoacoustic modeling of the sea floor", J. Acoust. Soc. Am. 68(5), 1313-1340.
[27] Kibblewhite , A. C., (1989): "Attenuation of sound in marine sediments: A review with emphasis on new low-frequency data", J. Acoust. Soc. Am. 86(2), 716-738.
[28] Stoll,R. D., (1989): Sediment Acoustics, Springer-Verlag, New York.
[29] Austin, J. A., Davies, T. A., Dean, D.F., Kessinger , W. P., Lagoe, M. B., Stoffa, P. L., Wiederspan, M., Ewing, J. I., Franks, E., Milliman, J. D. and Young, E., (1990) : "Huntec 3-D Survey On The Outer Continental Shelf Off New Jersey", ONR Progress Report, Code 1125 OA, Office Of Naval Research, Arlington, Va. 22203.
[30] Davies, T. A., Austin, J. A., Lagoe, M. B., and Milliman, J. D., (1992): "Late Quaternary sedimentation off New Jersey: New Results using 3-D seismic profiles and cores", Marine Geology, 108, 323-343.
[31] Stoll, R.D., Bryan, G.M., Mithal, R. and Flood,R. (1991): " Field experiments to study seafloor seismoacoustic response", J. Acoust. Soc. Am. 89(5), 2232-2240.
[32] Yamamoto,T. , Rogers, A., and Trevorrow, M., (1991): " Experimental verification and application of the bottom shear modulus profiler (BSMP) method", Oceans ' 91, Proceedings of the IEEE, IEEE, 345 E 47th St. New York.
[33] Trevorrow, M. V. and Yamamoto, T. (1991)." Summary of marine sedimentary shear modulus and acoustic speed profile results using a gravity wave inversion technique", J.Acoust. Soc. Am. 90(1),441-455.
[34] Schmidt, H., (1987): " SAFARI: Seismo-Acoustic Fast Field Algorithm For Range Independent Environments", SACLANT ASW Research Centre, I-19100 La Spezia, Italy.
[35] Jensen, F. B. and Ferla, M. C. (1979): " SNAP: The SACLANTCEN Normal-Mode Acoustic Propagation Model", Rep. SM-121, SACLANTCEN ,La Spezia, Italy.
[36] Porter, M. and Reiss, E.L., (1984): " A numerical method for ocean-acoustic normal modes", J. Acoust. Soc. Am. 76(1),244-252.
[37]Lee, D. and McDaniel, S.D., (1988): "Ocean Acoustics by Finite Difference Methods", Comput. Math. Applic. 14(5), 305-423.
[38] Collins, M.D. and Westwood, E. K., (1991): "A higher-order energy conserving equation for range dependent ocean depth, sound speed and density", J. Acoust. Soc. Am. 89(3), 1068-1075.
[39] Williams Jr., A.O., (1960): " Some effects of velocity structure on low-frequency propagation in shallow water", J. Acoust. Soc. Am.32(3), 363-371.
[40] Rogers, A.K., Yamamoto, T.,and Carey W. (1993): " Experimental investigation of sediment effect on acoustic wave propagation in the shallow ocean", J. Acoust. Soc. Am. 93(4, Pt.1), 1747-1761.
[41] Cederberg,R.J., Siegmann,W.L., Jacobson,M.J., and Carey,W.M., (1993): " Predic-tability of acoustic intensity and horizontal wave numbers in shallow water at low frequencies using parabolic approximations", Jour. Acoust. Soc. Am. 94(2).
[42] Wengrovitz, M. S. ,Oppenheim, A. V. and Frisk, G. V. (1987): "Reconstruction of complex-valued propagating wave fields using the Hilbert-Hankel transform," J. Opt. Soc. Am. 4(1),247-266.
[43] Yen, N., and Carey, W. M., (1989): "Application of synthetic-aperture processing to towed-array data", J. Acoust. Soc. Am. 86(2), 754-765. (See also W. M. Carey and N. Yen, " The formation of a synthetic aperture with towed hydrophones" NORDA Pub. SP40:84:13, 38 pp., 1984, available DTIC; also J. Acoust. Soc. Am. 75(s1),S62-3(A)).
[44] Williams, Jr., A. O.,(1976): " Hidden depths: Acceptable ignorance about the ocean bottoms," J. Acoust. Soc. Am. 59, 1175-1179.